11/27/85

MASTER

BNL 37500
OG 872

CONF-8511161--1

JAN 29 1986

Neutrino Electron Scattering at LAMPF

D. Hywel White
Department of Physics
Brookhaven National Laboratory
Upton, NY 11973

BNL--37500

DE86 005692

Talk given at LAMPF User's Meeting Nov. 2, 1985

DISCLAIMER

This report was prepared as an account of work sponsored by an agency of the United States Government. Neither the United States Government nor any agency thereof, nor any of their employees, makes any warranty, express or implied, or assumes any legal liability or responsibility for the accuracy, completeness, or usefulness of any information, apparatus, product, or process disclosed, or represents that its use would not infringe privately owned rights. Reference herein to any specific commercial product, process, or service by trade name, trademark, manufacturer, or otherwise does not necessarily constitute or imply its endorsement, recommendation, or favoring by the United States Government or any agency thereof. The views and opinions of authors expressed herein do not necessarily state or reflect those of the United States Government or any agency thereof.

DISTRIBUTION OF THIS DOCUMENT IS UNLIMITED

The Standard Model

A major accomplishment in elementary particle physics in the last fifteen years has been the success of the electroweak model of Glashow, Weinberg, and Salam in describing the unification of the electromagnetic and weak forces. The theory explains the experimental facts within the precision with which they are known in terms of a single phenomenological parameter. Many deeper uncertainties remain, particularly the origin of the masses of the intermediate vector bosons, but here we shall consider the limits of applicability of the standard model assuming that verifying the theory is a worthwhile goal and that exposing limitations of the theory may cast light on the deeper aspects, which are yet speculative.

The theory is described below from an experimenter's point of view, with heavy emphasis on the observables, including a summary of the present experimental situation. The electroweak interaction is described by the symmetry $SU(2)_L \times U(1)$ implying two independent coupling constants for the two constituent groups g' and g, respectively. The charged current interaction has been known (for some time) in the form of β decay and is well described by the exchange of a W^+ or W^- with equal axial and polar vector coupling constants.

The group SU(2) implies a W° in a triplet coupling with the same strength as the charged W. The U(1) group describes a single boson B° with different coupling to the SU(2) triplet but which is mixed with the W° to give a photon

$$|\gamma\rangle = \frac{g|B^\circ\rangle + g'|W^\circ\rangle}{\sqrt{(g^2 + g'^2)}}$$

and

$$|Z^\circ\rangle = \frac{g|B^\circ\rangle - g'|W^\circ\rangle}{\sqrt{(g^2 + g'^2)}}$$

The electromagnetic coupling of $|\gamma\rangle$ is

$$e = \frac{gg'}{\sqrt{(g^2 + g'^2)}} \quad .$$

The Z° can be written

$$|Z^\circ\rangle = g/\cos\,\theta_W\,[\sqrt{1/2}|\Phi^\circ{}_1\rangle - \sin^2\theta_W|\Phi_{em}\rangle]$$

with Φ°_1, the eigenstate of the weak triplet and Φ_{em} the electromagnetic eigenstate illustrating the fact that the Z° contains an electromagnetic component as is observed in e^+e^- collisions, for example.

At this stage, there are two neutral particles in the laboratory with coupling constants that reflect the mixing between them. We may define

$$\tan\,\theta_W = g'/g \text{ and then } \sin^2\theta_W = e^2/g^2 \quad .$$

Symmetry Breaking

When spontaneous symmetry breaking is introduced, for example from a Higgs field, the W and Z acquire mass and the photon becomes massless. Then in a simple version of symmetry breaking with a Higgs doublet gives

$$m_W/m_Z = \cos\,\theta_W$$

and

$$\sin^2\theta_w = e^2/g^2 = 1 - m_W^2/m_Z^2 \quad .$$

The fact that the Z^o mass is different from the W mass allows a solution for the mixing angle θ_W, but to establish the scale of g and g′ we must use a charged current process, for example μ decay. With a charged current coupling constant G_μ, and appropriate phase space factor

$$\frac{1}{\tau_\mu} = \frac{G_\mu^2\ m_\mu^5}{192\pi^3}$$

from the rate of decay of the muon, G_μ can be separated from the phase space contributions. We will be concerned below with radiative corrections to weak processes and muon decay is no exception; the corrections to first order in α are written below together with their numerical values. Then the muon lifetime of 2.197 μsec gives $G_\mu = 1.16635 \times 10^{-5}$ GeV[1].

$$(1 - 8m_e^2/m_\mu^2)(1 - 3/5\ m_\mu^2/m_W^2 + \alpha/2\pi(25/4 - \pi^2)(1 + 2\alpha/3\pi\ \ln(m_\mu/m_e)$$

$$0.99981 \qquad\qquad 0.99159 \qquad\qquad 1.00383$$

The SU(2)xU(1) theory with symmetry breaking gives an explicit relation for m_W.

$$m_W = \frac{\pi\alpha}{2G_\mu \sin^2\theta_W}^{1/2} = \frac{37.281}{\sin\theta_W}$$

and

$$m_Z = \frac{m_W}{\cos\theta_W} \quad .$$

Radiative Corrections

The masses of W and Z are generated by spontaneous symmetry breaking but with contributions from diagrams like

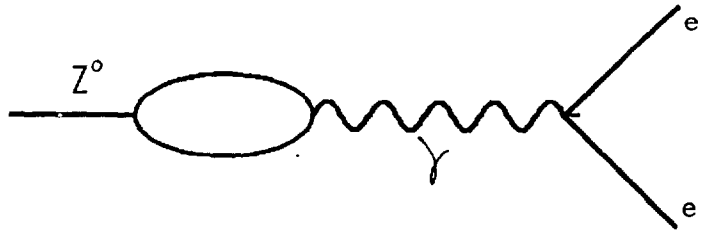

Fig. 1

These diagrams potentially contribute significantly, for example when the SU(2) x U(1) is embedded in the group SU(5) as an attempt at grand unification, then a prediction for $\sin^2\theta_w$ emerges as 3/8. Diagrams like that above contain loops from the grand unifying particles and generate substantial radiative corrections giving

$$\sin^2\theta_w^{exp} = \frac{3}{8} \left(1 - \frac{109\alpha}{18\pi} \ln(m_X/m_W)\right)$$

estimating m_X from the measured value of $\sin^2\theta_w$ gives $m_X \simeq 1.3 \times 10^{14}$ GeV. This approach has the difficulty that the predicted mass of m_X in turn implies a proton lifetime which is in conflict with the upper limits $\tau_p > 2.5 \times 10^{32}$ years from IMB and Kamioka. However, the point remains that the relation between $\sin^2\theta_w$ and the W and Z masses depend on contributions from radiative corrections. Define the sum of radiative contributions to the W mass as $(1-\Delta r)$, then

$$m_W = \frac{37.281}{\sin\theta_W \sqrt{(1-\Delta r)}} = \frac{38.64}{\sin\theta_W}$$

with

$$\Delta r = .069 \quad .$$

The mass of the W determined from the average of UA1 and UA2 is 81.8 ± 1.5 GeV, which yields $\sin^2\theta_W = 0.223 \pm 0.008$. The expression above

$$\sin^2\theta_W = 1 - m_W{}^2/m_Z{}^2$$

can be used to define $\sin^2\theta_W$ as an experimental quantity which gives

$$m_Z = \frac{m_W}{\cos\theta_W} = \frac{77.30}{\sin 2\theta_W} \quad .$$

The measured Z mass from the same two experiments

$$m_Z = 92.6 \pm 1.7 \text{ GeV}$$

gives $\sin^2\theta_W = 0.225 \pm 0.011$. Returning to the definition of e

$$\frac{e^2_{exp}}{g^2_{exp}} = \left(1 - \frac{m_W^2}{m_Z^2}\right) \qquad \left(1 - 2\,\frac{\delta e}{e}\,..\right)$$

experimental quantities $\qquad (1 + \Delta r).$

e_{exp} is potentially variable depending on the process by which it is measured, that is at the masses of W and Z or in the scattering processes. δe expresses this variation with contributions from leptonic, hadronic, and bosonic loops. Numerically,

$$\Delta r = \underset{\text{leptonic}}{0.033} + \underset{\text{hadronic}}{0.033 \pm 0.003} + \underset{\text{bosonic}}{0.003}$$

The leptonic corrections assume three generations at the known masses. The hadronic corrections similarly assume three generations with a top mass at $\simeq$ 36 GeV. The correction is approximately logarithmically dependent on this mass. Higher mass generations would increase this correction substantially with the error $\pm$ 0.003 reflecting a reasonable uncertainty on the mass of the top quark. The bosonic correction comes from W loops and a contribution from the Higgs. To estimate this correction, a Higgs mass equal to the Z was used, clearly uncertain at this time.

When radiative corrections are calculated for scattering processes, an extra diagram appears.

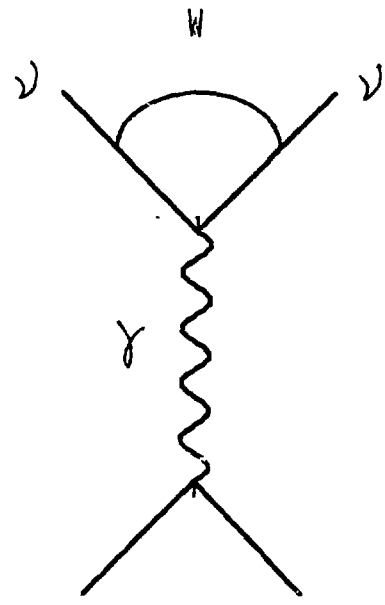

Fig. 2

This term is roughly equal and opposite in sign to the sum of corrections to the mass terms above so that little numerical correction is required for neutral current processes like ν_μ-e scattering, at least in the context of the standard model with the definition of $\sin^2\theta_w$ above.

Scattering from Hadrons

The ratio of scattering of neutrinos from hadrons in the neutral current (Z exchange) and charged current (W exchange) channels depends on $\sin^2\theta_w$. In deep inelastic scattering with four momentum transfer Q^2 to the lepton

$$R_\nu = \frac{\sigma_{nc}}{\sigma_{cc}} = \rho^2_{\nu n} \left[1/2 - \kappa(Q^2)\sin^2\theta_w + \frac{20}{27}\kappa^2(Q^2)\sin^4\theta_w\right]$$

$$= 0.31$$

$\kappa(Q^2)$ is the radiative correction to the neutral current cross section and is weakly dependent on Q^2; a typical value is 1.006. The charged current cross section has also a radiative correction which is somewhat larger and is included in $\rho_{\nu n}{}^2 \simeq 0.98$. These experiments have the advantage of a copious event rate although the systematic uncertainties have given trouble, which has been reflected in different values of $\sin^2\theta_w$ from different experiments. The analysis assumes that the parton model is applicable to the structure and this may be a concern, although the cross section ratio measurement helps to reduce the systematic uncertainty. A present world average is

$$\sin^2\theta_w = 0.223 \pm 0.008.$$

A conceptually similar measurement is made in $\nu_\mu p$ elastic scattering at Brookhaven. Form factors are measured in electron scattering and in ν_μ quasi elastic scattering. The cross section is then understood with $\sin^2\theta_w$ as a parameter and a possible induced isoscalar contribution. The level of systematic understanding does not make it competitive in accuracy at this time with deep inelastic scattering, but $\sin^2\theta_w = 0.220 \pm 0.016 \begin{smallmatrix}+0.023\\-0.031\end{smallmatrix}$.

The Z° is coupled to e^+e^- and the weak electromagnetic interface may be observed at an e^+e^- collider. Parity violation in the weak interaction induces an asymmetry in the production of μ pairs, which may be expressed as

$$\frac{d\sigma}{d\cos\theta} = \frac{\pi\alpha^2}{2S} R_{\mu\mu} \left(1 + \cos^2\theta + 8/3\ A_{\mu\mu} \cos\theta\right) \quad .$$

In a recent experiment at PEP, MAC has quoted $R_{\mu\mu} = 1.001$ and $A_{\mu\mu} = -0.063$. $A_{\mu\mu}$ is subject to radiative corrections of the same general type with a value of 0.0314 ± 0.006. This experiment basically measures the interference of the electromagnetic amplitude with the tail of the Z^o and will be expected to improve in accuracy as the C.M. energy of colliders improve. Ultimately, with SLC or LEP, the measurement of the Z^o mass will lead to the greatest precision at an e^+e^- collider. Presently, the value of $\sin^2\theta_w$ is typically

$$\sin^2\theta_w = 0.22 \begin{smallmatrix} + 0.05 \\ - 0.04 \end{smallmatrix} \ .$$

Neutrino-Electron Scattering

ν_e-e scattering, E225, is being measured at LAMPF and this group has an interim publication of their data. The radiative corrections are comparable to the charged current corrections discussed in the section on deep inelastic scattering above. At the present time, this experiment has determined the sign of the interference between the charged and neutral currents (it is destructive) and have a value of $\sin^2\theta_w$

$$= 0.21 \begin{smallmatrix} + 0.08 \\ - 0.12 \end{smallmatrix} \begin{smallmatrix} + 0.05 \\ - 0.07 \end{smallmatrix}$$

ν_μ-e scattering is being measured in two experiments, CHARM at CERN and E734 at Brookhaven. The radiative corrections are negligible in these scattering experiments because of the accidental cancellation discussed above. This cancellation depends on the particles that are assumed to contribute to the

loops in the diagrams that are considered, so that the fact that the radiative corrections are small is particularly true for the standard model.

In the published literature

$$\text{CHARM} \quad \sin^2\theta_W = 0.215 \pm 0.032 \pm 0.013$$

$$\text{BNL} \quad \sin^2\theta_W = 0.209 \pm 0.029 \pm 0.013 \ .$$

In CHARM II and in further running for BNL, the combined error may be reduced to 0.020.

A New LAMPF Experiment

The preceding discussion underscores the need for a really precise measurement of $\sin^2\theta_W$ in the scattering mode. The measurement of the Z and W masses will provide an alternate determination and the difference in $\sin^2\theta_W$ from the measurement of the masses squared and from scattering is .015 in the standard model. This is near the limit for present (and near future) measurements. So as the statistical precision improves, the systematic understanding of the experiments is becoming a limiting feature.

A group at LAMPF is proposing an experiment that combines excellent statistical precision with the potential for low systematic uncertainty. The proposal is to measure the ratio

$$R = \frac{\sigma(\nu_\mu e)}{\sigma(\nu_e e) + \sigma(\bar{\nu}_\mu e)} \ .$$

In terms of the standard model $SU(2)_L \times U(1)$

$$R = \frac{3}{4}\,\frac{1 - 4\sin^2\theta_W + 16/3\sin^4\theta_W}{1 + 2\sin^2\theta_W + 8\sin^4\theta_W}$$

when $\sin^2\theta_W$ increases, $\sigma(\nu_\mu e)$ increases and both $\sigma(\bar{\nu}_\mu e)$ and $\sigma(\nu_e e)$ decrease, the last because the charged and neutral currents interfere destructively. There is an immediate gain, therefore, in measuring this ratio over the measurement of the individual rates. Each reaction has a similar signature, namely that the recoil electron has a small angle to the incident neutrino direction. The $\nu_e e$ cross section is about six times either of the $\nu_\mu e$ cross sections, which are about equal. To measure the ratio, ν_μ must be distinguished from ν_e and $\bar{\nu}_\mu$. The lifetime of the pion is 25ns and the μ 2200 ns. The proposal uses the proton storage ring (PSR) to compress a LAMPF pulse to 270 ns. We show in Fig. 3 a spill from the PSR and the time-dependent neutrino fluxes from the decay chains

$$\pi^+ \rightarrow \mu^+ + \nu_\mu$$

$$\mu^+ \rightarrow e + \nu_e + \bar{\nu}_\mu \ .$$

There are equal numbers of ν_μ, ν_e, and $\bar{\nu}_\mu$ integrated over all three, but within the 270 ns spill the ratio

$$\frac{N_{\nu_e}}{(N_{\bar{\nu}_\mu} + N_{\nu_e})} = 0.06 \ .$$

The Detector

Experiments using a stopped pion source have been considered at LAMPF at least since 1969. The $\nu_e e$ experiment that is presently running demonstrates the feasibility of the idea. The use of the PSR for time separation of ν_μ and $\nu_e, \bar{\nu}_\mu$ has the disadvantage that the available flux is reduced compared to the existing beam stop. More events are required to reach the precision that is required to impact physics in the next decade. It has been recognized at LAMPF that a new detector technology has emerged that makes very large neutrino detectors feasible financially. The detector we refer to is the water cherenkov detector for electrons in which enough cherenkov photons are collected in enough separate phototubes that reconstruction of the energy and direction is possible. A prototype of this technology is operating at Kamioka looking for proton decay in which appropriate energy and angular resolutions have been demonstrated. The number of cherenkov photons produced by a charged particle is

$$N = \frac{2\pi\alpha}{C} \left(1 - \frac{1}{n^2\beta^2}\right) \Delta\ell \ \delta\nu$$

$n = 1.344$ for water and $\beta \simeq 1$ for electrons. For a typical phototube and water as an absorbing medium $\Delta\nu \simeq 5.7 \times 10^{14}$ sec^{-1}.

Assuming a reasonable quantum efficiency of 0.1 averaged over angle, the number of photoelectrons

$$N_e = f \times 10/\text{MeV}$$

where f is the fractional coverage of photocathode in the detector. The angle of the cherenkov cone

$$\cos\Theta = 1/n\beta \ , \ \Theta = 41.4^\circ \text{ for } \beta = 1 \ .$$

The radiation length in water is 36 cm and a typical multiple scattering angle for a 20 MeV electron is about 15°. For 25% photocathode coverage a 20 MeV electron yields 50 photoelectrons. The angular resolution is such as to largely preserve the ring structure of the cherenkov light and the number of photoelectrons should produce energy resolution at the 20% level. The cost of the photomultiplier and electronics is a major constituent of the detector and for a point source the optimal distribution of detecting elements is on the surface of a sphere. A highly schematic view of a possible detector is shown in Fig. 4. The proton beam is stopped in the center of an iron hemisphere that is thick enough to absorb the neutron flux from the target. The phototubes are arranged on the surface of a hemisphere of 17 m radius. This gives an effective thickness of about 9 m for the water in which neutrino interactions can be detected; the interaction rate is proportional to this thickness. The cherenkov cone of 41° will occasionally impinge on the area outside the hemisphere, so that phototubes are also deployed on the iron and also on the flat surface. These phototubes also detect light from events in which the angle of scatter of the secondary electron is large enough that the information of the neutrino direction is lost. Cosmic rays also will produce electrons from the decay of muons that shop in the detector that will frequently be detected outside the hemisphere. Signal events will appear to come from the target and a scheme has been suggested to enhance the light coverage for these events by mounting mirrors between the phototubes on the hemisphere and reflecting light back on to the iron hemisphere and collecting these photons there. This scheme will have to be studied carefully to avoid degradation of the cherenkov pattern by

additional reflections. The cosmic ray rate is large and a veto will need to be provided. The water outside the hemisphere is envisaged as a suitable medium to detect incoming muons and some of the hadrons.

In Fig. 5 we show two Kamioka cosmic ray events. In the top event, the muon ring is very clear, with a decay electron. In the bottom event, the muon is not visible but the decay electron is obvious. These electrons are approximately the quality of events that would appear in a LAMPF detector of this type. Electrons from decaying stopped muons have the well known Michel spectrum, this spectrum measured at Kamioka is shown in Fig. 6, illustrating the accuracy of the Monte Carlo model of the data. At this level of detail, the experiment seems feasible with a high level of cancellation of systematic effects in numerator and denominator of the cross section ratio. The principal uncertainty is in the energy resolution function because the secondary electron spectrum is different in numerator and denominator so the threshold behavior of the electron detection efficiency must be well known.

Photomultiplier Cost Estimate

The photomultipliers and associated electronics form the single most expensive component of the experiment. As an example, we have chosen the Hamamatsu 20" tube used at Kamioka. The active area of this tube at 25% coverage means that each tube takes care of an area of 0.66 m^2. The table below gives an estimate of the area of the detector components.

Area of outer hemisphere 17 m radius	1,816 m^2
Area of inner hemisphere 7 m radius	308 m^2
Area of plane bottom	754 m^2
This translates into:	
Outside hemisphere (25% coverage)	2,764 tubes
Inside hemisphere (25% coverage)	470 tubes
Plane bottom (10% coverage)	470 tubes

The total number of tubes is 3,694 and at 1.5 K$ per channel this is 5.54 M$. The mirrors on the outer hemisphere focusing on the inner hemisphere give a total of 40% light collection for νe electrons with 60% coverage.

Counting Rate Estimate

It is assumed that the experiment might run for three years with 130 days equivalent for each year. For the geometry of Fig. 3 and 100 μA of beam,

Total number of $\nu_\mu e$ events	14,270
Assume 60 μA is delivered on average	8,560
Electron energy cut at 12 MeV	4,400
85% detector operating efficiency	3,730
80% pattern recognition efficiency	3,000

This translates into an error on $\sin^2\theta_W$ of ± 0.0024.

Background

The residual cosmic ray and beam associated backgrounds are estimated below for the electron range between 10 and 60 MeV. E225 has been used as a model so that these estimates are completely empirical, and may improve with more caareful shield engineering. The numbers of background events are to be compared with 8 $\nu_\mu e$ events/day after all cuts described above.

	Beam Associated	Stopping Cosmic Ray
Background in E225/day	0.5	100
Increase for lower energy threshold: 20 MeV → 10 MeV	1.0	150
Scaling to larger detector Neutrons by inside surface area Cosmic Rays by projected area	50	15000
Reduction for addition 1.5 m Fe m shield	5	15000
Forward angle cut	.25	750
PSR duty factor	.25	2.5×10^{-3}
Scale factor for 60 μA current	.025	2.5×10^{-3}

The beam associated background is dominant and represents a signal/background of 300:1. This may be compared with about 4:1 in the BNL experiment.

Conclusion

We all agree that the standard model of Glashow, Weinberg, and Salam is a good description of the experimental world at the present level of accuracy. The first non-trivial corrections to the theory occur at the one-loop level and because they are different in their contributions to vector boson mass and in

scattering, the two classes of measurements offer a serious test of the theory and of the particles that are assumed to contribute via the appropriate loops to the radiative corrections. The difference of the expected radiative corrections at the mass squared of Z and at the Q^2 of neutrino electron scattering is .069, which reflects into an apparent difference in $\sin^2\theta_W$ of .015. A group has been studying an experiment that could yield an accuracy of 0.0025 in $\sin^2\theta_W$ putting this section of the theory to a significant test.

Acknowledgements

In preparing this talk, I have exploited the patience of Bill Marciano, my knowledge of the radiative corrections is almost entirely due to him. Many people at LAMPF have contributed ideas and effort to the exploration of a convincing experimental scenario and detector design. I have borrowed their ideas extensively; some of them are Bob Burman, Herb Chen and the people at Irvine, Roger Carlini, Joey Donahue, and Vern Sandberg. Gerry Garvey has urged us on and continues to do so. I expect that these people and others will produce a detector design that can be used to do this exciting physics.

This research has been supported by the U.S. Department of Energy under Contract No. DE-AC02-76CH00016.

Neutrino Source

PSR produces pulses of protons of
270 ns duration into a beam stop target

π^+ stop and decay from rest
π^- are absorbed

Decay chains:

$$\pi^+ \rightarrow \mu^+ + \nu_\mu$$
$$\hookrightarrow e + \nu_e + \bar{\nu}_\mu$$

Equal numbers of ν_μ, ν_e, and $\bar{\nu}_\mu$.

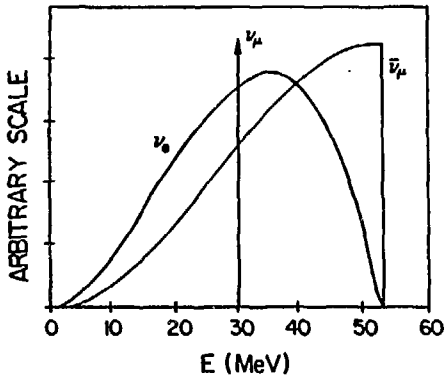

Within the 270 ns spill $\frac{N_{\nu_e}}{N_{\nu_\mu} + N_{\nu_e}} = 0.06$

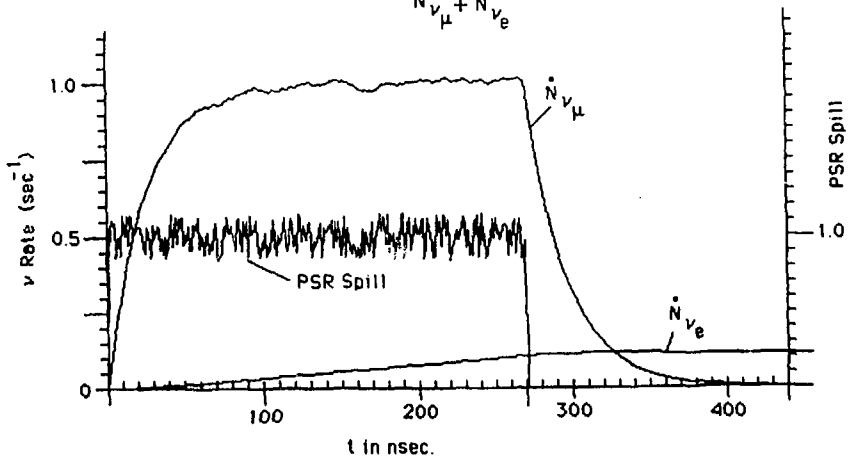

Fig. 3

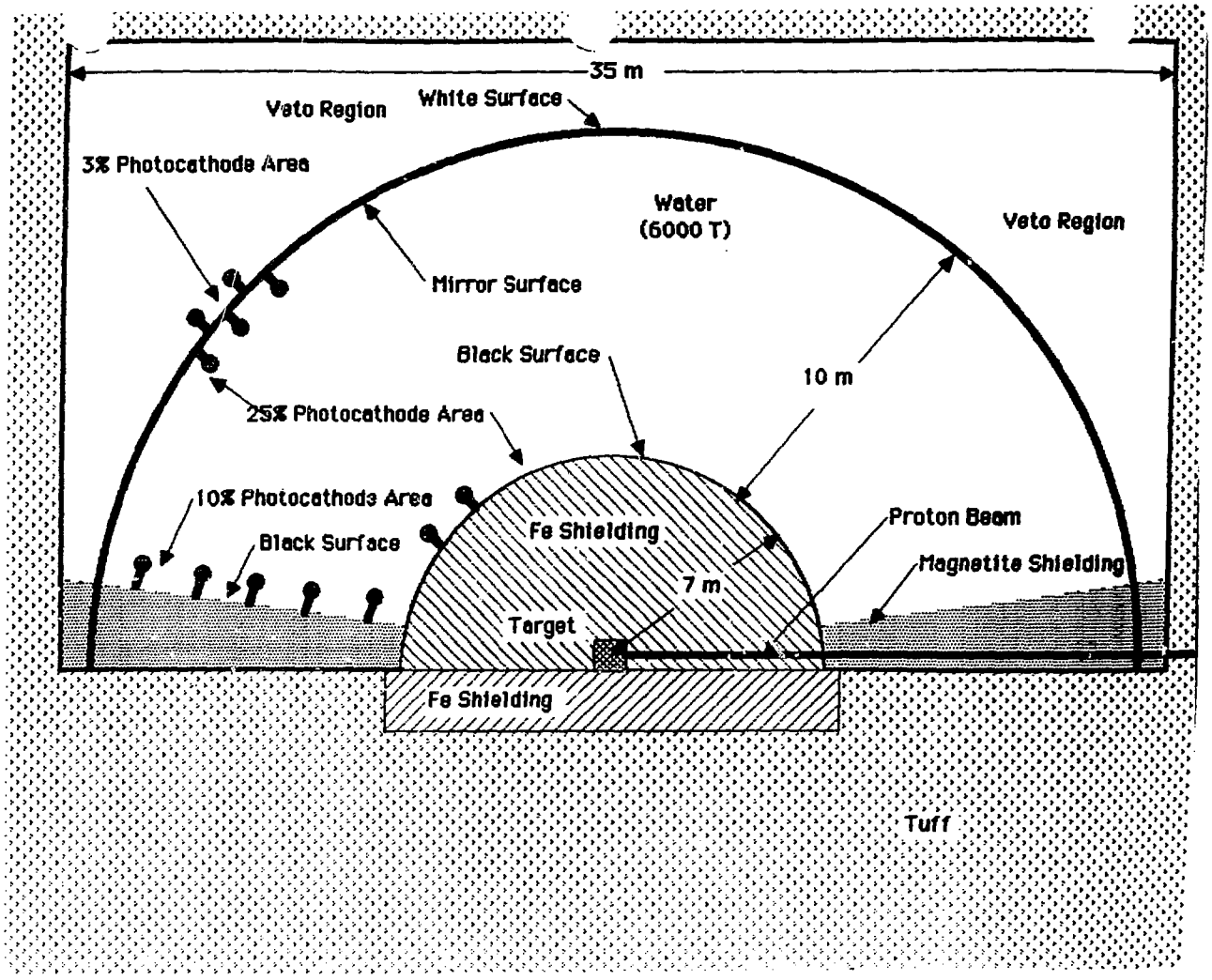

Fig. 4. A version of the Los Alamos neutrino experiment. The steel hemisphere is for neutron shielding, phototubes are mounted on a hemispherical support immersed into water.

REPRODUCED FROM
BEST AVAILABLE COPY

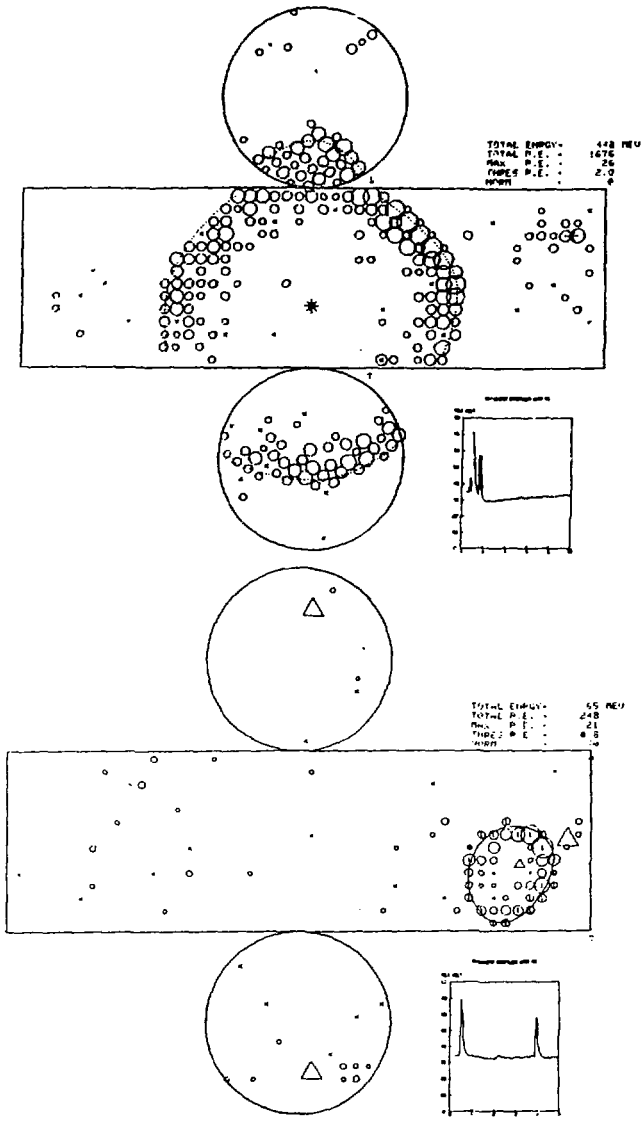

Fig. 5. Examples of two low-energy events as seen in the Kamioka detector. The top event is a stopping muon with it's Michel decay electron seen as the small circle on the right. The second, is a muon decay ($\mu \rightarrow e$) in which only the electron is seen. These are projections of the PMT's hit pattern onto an unrolled cylinder. The "top" and "bottom" of the cylinder are also shown. Particle identification is possible from the diameter and "fuzziness" of the rings. Incident momentum is determined from the number of photoelectrons generated.

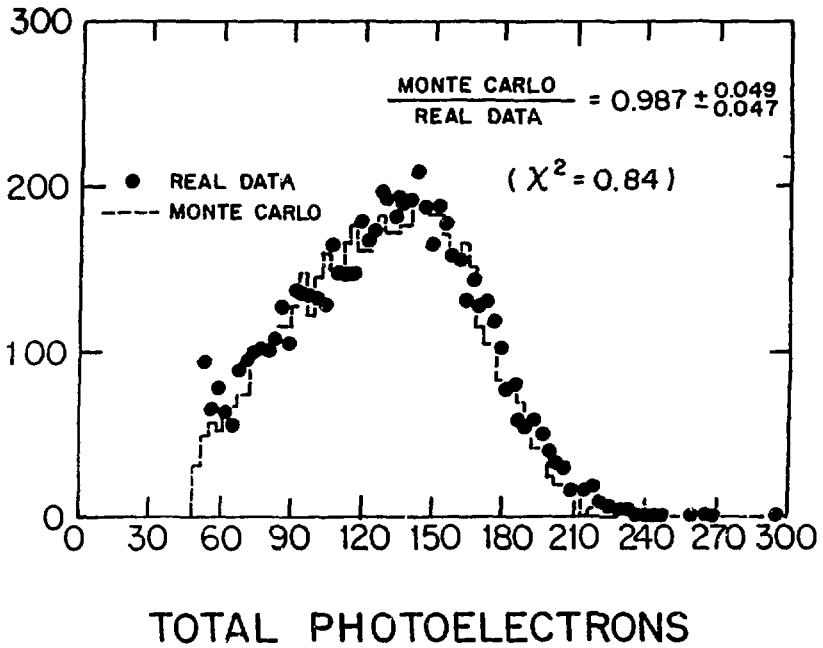

Fig. 6. The Michel electron spectrum as seen by the Kamioka imaging water Cherenkov detector.